NATIONAL ADVISORY COMMITTEE FOR AERONAUTICS

ADVANCE CONFIDENTIAL REPORT

Special Report # 211

WIND-TUNNEL INVESTIGATION OF SEVERAL FACTORS AFFECTING THE PERFORMANCE OF A HIGH-SPEED PURSUIT AIRPLANE WITH AIR-COOLED RADIAL ENGINE

By Carl J. Wenzinger
Langley Memorial Aeronautical Laboratory

November 1941

WIND-TUNNEL INVESTIGATION OF SEVERAL FACTORS AFFECTING THE PERFORMANCE OF A HIGH-SPEED PURSUIT AIRPLANE WITH AIR-COOLED RADIAL ENGINE

By Carl J. Wenzinger

SUMMARY

An investigation was made in the NACA 19-foot pressure wind tunnel of a 0.4-scale model of an existing pursuit airplane to obtain the experimental information required to indicate the improvements necessary to produce an airplane capable of reaching a speed in excess of 400 miles per hour at an altitude of 20,000 feet with an air-cooled engine of 1000 horsepower output. Modifications to the model included a low-drag wing, changes in the fuselage shape, a high-speed cowling, and certain other improvements. The scale of the tests was increased by operating the tunnel under pressure when it was considered advisable, thus giving Reynolds numbers up to full scale for the landing condition.

Based on the results of the tests it was found that, by use of the NACA low-drag sections for the wing, important reductions in wing drag and important increases in compressibility speeds were obtained, the lift and stalling characteristics were similar to those of conventional wings, and the action of simple split flaps in increasing the lift was about the same. The propeller slipstream caused an increase in the drag of that portion of the low-drag wing in the slipstream to a value about the same as that of a conventional wing without slipstream.

The NACA high-speed cowling arrangement appears to be satisfactory up to speeds of more than 500 miles per hour at high altitudes before critical compressibility effects are encountered. In addition, propulsive efficiencies appear to be increased by use of this cowling at high values of V/nD compared with the efficiencies obtained with cowling C. The aerodynamic advantage of placing wing guns within the wing is indicated.

INTRODUCTION

In connection with the existing national emergency and as part of the national defense program, the NACA is conducting investigations to determine the improvements in performance that can be achieved through the application of recent wing, cowling, and fuselage research to single-engine and multiengine military airplanes.

The investigation described in this paper was started in the summer of 1940 and was proposed to obtain some experimental information concerning the possible improvements to be obtained by the application of the results of the previously mentioned researches to a typical pursuit-type airplane. In particular, it was hoped to indicate the improvements necessary to produce an airplane capable of reaching a speed in excess of 400 miles per hour at an altitude of 20,000 feet with an air-cooled radial engine of 1000 horsepower output, such as the R-1830. This aim, of course, is modified from time to time in the light of findings from the present war, but it is believed desirable to make available in a short concise report some of the more outstanding results of the investigation that may be used as a guide to further development.

As a starting point, an existing experimental airplane was chosen as one representative type of high-performance pursuit airplane. A 0.4-scale smooth model without protuberances was built, and its aerodynamic characteristics were used to establish a basis from which possible improvements could be judged. Modifications were then made, usually one at a time, to incorporate the proposed improvements. The modifications included principally a low-drag wing, a change in the fuselage shape, a high-speed cowling, and certain other improvements. All tests were carried out in the NACA 19-foot pressure wind tunnel, at Langley Field, Va. The scale of the tests was increased by operating the tunnel under pressure when it was considered advisable, thus giving Reynolds numbers up to full scale for the landing condition.

MODELS AND APPARATUS

The models were all constructed of laminated mahogany, reinforced with metal where required. The exposed surfaces were filled, then sprayed with lacquer, and finished by

rubbing with No. 400 water cloth in a direction parallel to the wing chord. The finish thus secured was such as to be classified as "aerodynamically smooth."

The resistance of the engine to air flow through the cowling was simulated by a perforated plate of such design that its conductance could be adjusted to approximate that of the full-scale engine installation. For some of the tests, dummy cylinders were also attached to the plate to represent more exactly the actual engine installation.

When tests of powered models were required, a three-blade, 4-foot-diameter propeller, which has blades of Clark Y section mounted in an adjustable-pitch hub, was used. This propeller is similar to the full-scale Hamilton Standard propeller 6101. For these tests, the blades were set at angles of 45°, 50°, and 55° at 0.75 of the tip radius.

The propeller was driven by a water-cooled alternating-current induction motor capable of developing 60 horsepower at 5000 rpm. Current was supplied to the motor by a variable-frequency motor-generator set, and speed control was obtained by varying the frequency. The output torque of the motor was determined from a calibration of torque against active current. The motor revolution speed was measured with a condenser-type tachometer.

The models were mounted on the standard supporting system of the balance in the NACA 19-foot pressure wind tunnel. (See fig. 1.) Two main supports were used for the wing, one on each side of the fuselage, and a single tail support was used by which the angle of attack was changed. Six-component measurements of aerodynamic forces and moments were made and recorded by an automatic electric recording balance.

TESTS

All tests were made with the tunnel test section in the closed-throat condition and with the air pressure in the tunnel either at atmospheric or at 35 pounds per square inch absolute, depending upon the type of test and the Reynolds number desired

The angle-of-attack range covered, in general, from below zero lift to beyond maximum lift. Observations of the stalling characteristics of the wings were made by

noting the action of wool tufts attached to the upper surface of the wing.

The section profile drag of the wing when operating in the vicinity of the high-speed lift coefficient was obtained from measurements of the momentum loss in the wing wake. Pressure measurements over cowling and fuselage were made by the use of pressure orifices installed in the model, or by the use of nice. Measurements of air flow through the cowling were made with total-pressure and static tubes.

When required, determinations were made of the lift, drag, and aerodynamic interference effects of the model supports.

RESULTS AND DISCUSSION

Coefficients

All results are given in the form of absolute coefficients. Lift, drag, and pitching moments have been corrected for the tares due to the model supports, and drag and angle of attack have been corrected for jet-boundary interference effects. The coefficients and symbols are defined as follows:

C_L	lift coefficient	(L/qS)
C_D	drag coefficient	(D/qS)
c_{d_o}	section profile-drag coefficient	(d_o/qc)
C_m	pitching-moment coefficient	$(M/qc^2\ b)$
C_T	propulsive thrust coefficient	$(T-\Delta D)/\rho n^2\ D^4)$
C_P	power coefficient	$(2\pi Qn)/(\rho n^3\ D^5)$
$\frac{V}{nD}$	advance-diameter ratio of propeller	
η	propulsive efficiency	$\left[\frac{(T-\Delta D)V}{2\pi Qn}\right]$

where

L lift

D drag

d_o section profile drag by momentum method

ΔD change in model drag due to propeller slipstream

M pitching moment about model support

T thrust of propeller in presence of body (shaft tension)

Q aerodynamic torque of propeller

q dynamic pressure of air stream $(\frac{1}{2} \rho V^2)$

ρ mass density of air

V velocity of free stream

D diameter of propeller

n propeller revolution speed

b wing span

c wing chord

S wing area

and

α angle of attack of wing root chord

β propeller blade angle

δ_f flap deflection

Maximum Lift and Stalling Characteristics

Because of the possibility of obtaining lower drags by the use of a wing having NACA low-drag airfoil sections, such a wing was built for the model. At the time this wing was built there was some question as to the maximum lift obtainable with the low-drag sections, and this wing was made with a somewhat larger area and span than the wing originally used on the airplane. Figure 2 shows the arrangement of the basic model with wing having conventional airfoil sections (modified NACA 230 section); figure 3 shows the model with the new wing having NACA low-drag airfoil sections.

The new wing has a symmetrical airfoil section at the wing root with a thickness of 18 percent of the airfoil chord and is of the NACA 66 family; the design lift coefficient for the low-drag range is 0 with a variation of ±0.2. The section at the wing tip is cambered with a thickness of 15 percent and is of the NACA 67 family; its design lift coefficient is 0.13 with a variation of ±0.1. Outlines of the root and the tip airfoil sections and their ordinates are given in figure 4.

In order to improve the stalling characteristics of the wing, it was given a linear geometric twist of 2.15° from root to tip so that 1.5° of aerodynamic washout was obtained. Simple partial-span split flaps having chords 20 percent of the wing chord were included to obtain some data regarding the effectiveness of this type of flap when used with the low-drag wing in comparison with the effectiveness of the flap when used with the conventional wing. A few tests were also made with full-span split flaps.

The lift characteristics of the basic airplane model with conventional wing are plotted against angle of attack in figure 5 and the drag and the pitching-moment data are given in figure 6. Similar data for the same model but with low-drag wing are given in figures 7 and 8. The effects on the maximum lift coefficient of deflecting the simple split flap are indicated in figure 9 for the two different types of wing. Probably the most striking facts illustrated by the foregoing data are the similarity between the characteristics of the model with either type of wing and the possibility of obtaining equal maximum lift coefficients at the high flap deflections.

Surveys of the flow over the two types of wing were made by observing wool tufts attached to the upper surface of each wing. Sketches showing the progression of the stall are given for the conventional wing with the flap neutral in figure 10(a) and for the conventional wing with the partial-span flap down 60° in figure 10(b). Similar diagrams for the low-drag wing are given in figures 11(a) and 11(b).

The sketches for the conventional wing indicate that this wing would stall suddenly and with little warning. It should be noted, however, that a wing with conventional sections could be made that would stall in a manner considered satisfactory. The sketches for the wing with low-drag sections indicate a progressive stalling from root to

tip that should give sufficient warning before complete stall. These data indicate that a wing with low-drag sections can be designed to have desired stalling characteristics.

Effect of Propeller Slipstream on Wing Section Profile Drag

The drag of the low-drag airfoil sections appears to be considerably affected by surface smoothness and finish and by turbulence of the air flowing over the surface. Although the turbulence of the air in the 19-foot pressure wind tunnel is low compared with that of most wind tunnels, it appears to be not quite so low as that of free air, and the magnitude of turbulence increases somewhat with an increase in the test velocity. At low test velocities a good indication is given of the drag of the low-drag airfoil sections in this wind tunnel, and the values thus obtained provide a basis for some comparisons.

Measurements of the momentum loss in the wing wake were made to determine the section profile drag of both the conventional and the low-drag smooth wings without propeller slipstream. These measurements were made over a range of low lifts in order that the results obtained would correspond to those for a high-speed condition. The complete airplane model was used for these tests.

The section profile-drag coefficients are plotted for the conventional wing in figure 12 against distance from the center line of the fuselage. Two types of coefficient are given: one is based on the section chord at the point in question along the wing span; the other is based on the mean chord of the wing. The drag coefficient based on section chord will be seen to vary for the greater part of the wing span between the values of approximately 0.006 to 0.007, with peaks near the fuselage. These peak values are probably due to interference effects between the fuselage and the wing caused by a thickening boundary layer on the fuselage and earlier transition on the wing.

The data plotted in figure 13 are given for the wing with low-drag sections. The magnitudes of these section profile-drag coefficients vary from about 0.0035 to 0.0045 over most of the span, indicating a considerable reduction in the section drags compared with those of the conventional wing. Similar peak values also exist near the fuselage with the low-drag wing, as with the conventional wing.

Measurements with propeller operating were made to determine the effects of propeller slipstream on the section profile drag of the portion of the low-drag wing in the slipstream. The data obtained from these measurements are given in figure 14 for the condition of propeller operating at thrust equal to the drag of the model. The profile drag of the sections of the low-drag wing in the propeller slipstream is materially increased owing to the action of the slipstream, reaching values about the same as those of conventional sections without slipstream. A few measurements made with propeller idling indicate that the adverse effects are nearly as great as for the condition of propeller thrust equal to drag.

The results obtained show quite clearly that, in order to realize the full benefits of the low-drag wing sections, propeller slipstream over the wing surfaces should not be permitted. The desirability of the pusher propeller arrangement is therefore apparent if the full benefits available from these wing sections are to be obtained.

NACA Conventional Cowling C and NACA High-Speed Cowling

The form of cowling known as the NACA cowling C (reference 1) is in use on most airplanes at the present time but is known to be subject to compressibility effects at airplane speeds around 400 miles per hour at high altitudes. At speeds of about 430 miles per hour at 20,000 feet altitude, these effects become critical, and some other form of cowling becomes necessary. A cowling shape recently developed in the 8-foot high-speed wind tunnel served as the basis for a new practical high-speed cowling with critical compressibility effects delayed to well over 500 miles per hour at high altitudes.

Some tests were made during the course of the present investigation to obtain an indication of the relative merits of the NACA conventional cowling arrangement C (fig. 15) and of the new NACA high-speed cowling arrangement (fig. 16). In the high-speed cowling the cooling air enters the cowling through an opening ahead of the propeller, passes internally through an element of the cowling that rotates with the propeller and acts as a blower, and thence flows past the engine cylinders to the exit at the rear of the engine. Both types of cowling tested were so designed that all the cooling air required for the engine and its

accessories is taken in at the cowling entrance. A detailed description of these arrangements is given in reference 2.

Some pressure measurements were made over the nose of cowling C without propeller to determine the magnitude of the static pressures acting on the surface. The lowest pressure for the arrangement tested had a value $\left(\frac{p_o}{q} = -0.9\right)$ that corresponds to a critical Mach number $(M_{cr} = 0.62)$ and a critical speed of about 439 miles per hour at 20,000 feet altitude. Similar pressure measurements over the high-speed cowling gave values in all cases nearly equal to the free-stream static pressure. Other measurements of the pressures acting on the air-duct blister behind the rotating part were made with the cowling nose portion rotating without propeller at $V/nD = 2.71$. From these measurements, the lowest value of pressure $(p_o/q = 0.48, M_{cr} = 0.72)$ was found on the blister in its plane of symmetry at a point 9 inches back (model scale) of the trailing edge of the rotating nose.

With each of the two cowling arrangements, aerodynamic characteristics of the propeller were measured at three blade angles in the region of the high-speed flight operating condition. All values of propulsive efficiency presented are based on the drag of the aerodynamically smooth airplane model. The envelope efficiency curve obtained with the NACA cowling C is compared, in figure 17, with a similar curve obtained with the NACA high-speed cowling. The results indicate that, although the high-speed cowling increased η_{max} by only a small amount (2 percent) at $\frac{V}{nD} = 2.0$, this cowling increased η_{max} by approximately 10 percent at $\frac{V}{nD} = 3.0$.

The complete airplane model was tested with streamline fairing over the fuselage nose for each of the two cowlings to obtain an indication of the drag chargeable to these cowling and cooling arrangements. Comparison of the drag (at $C_L = 0.1$) of the complete model with streamline nose and of the model with cowling C and air flow indicates that cowling and air-flow effects in this case correspond to an increase in drag coefficient of 0.0012. For the case of the high-speed cowling, the cowling and air-flow effects increase the drag coefficient of the complete model by 0.0009.

Fuselage and Tail Surface

Two revised fuselage arrangements with a minimum of wetted area were investigated, one with a long body and one with a short body. The long body had tail surfaces that were smaller than those used with the short body; each fuselage and tail was designed to give approximately the same pitching moments. The fuselage shapes, in addition, were changed from that of the original fuselage in order to reduce the velocities in the region of the wing which in turn would decrease adverse interference effects on critical compressibility speeds. For a similar reason, the wing root section was changed at the same time from the NACA 66,2-018 section to the NACA 65,2-017 section. (See fig. 4.) Plan and elevation views of the model arrangements are shown in figures 18 and 19.

Some results of the drag measurements (without propeller) are summarized in the following table. Pitching-moment coefficients for the arrangements tested are given in figure 20.

Drag Coefficients of Models without Propeller

Model arrangement	C_D at C_L = 0.1
Complete model; air flow; long fuselage; tail on	0.0113
Complete model; air flow; short fuselage; tail on	.0112
Complete model; air flow; short fuselage; tail off	.0100
Complete model; no air flow; short fuselage; tail on; streamline nose	.0103

These data indicate practically no difference in the drag of the complete model at the high-speed lift coefficient (C_L = 0.1) with either the long or short body and the corresponding tail. Because of its smaller size, the model with short fuselage was used for the remainder of the investigation.

Pressure measurements over the wing-fuselage juncture indicated the measured pressures to be about the same as those of the wing alone. This condition reduces the induced velocities at the juncture due to the fuselage to zero and eliminates from that source adverse interference effects on critical compressibility speed. Thus, it appears feasible by proper consideration of junctures of wing and body to eliminate the adverse interference effects that are of main importance in the attainment of high airplane speeds.

Surface Irregularities

In order to obtain some indication of the effects of surface irregularities on the low-drag wing, tests were made with simulated arrangements. Retractable landing-gear cover plates (fig. 21) consisting of metal plates 1/16 inch thick were cut to the required shape and fitted to the lower surface of wing and fuselage. These plates were attached to the model by small flat-head nails closely spaced. Rudder and elevator sealed hinge joints (fig. 22) were simulated by metal strips 1/16 inch thick and 3/8 inch wide nailed to the respective tail surfaces at the hinge axes and faired to the surface at the upstream edges. Flush door, canopy, and inspection plate joints without leakage (fig. 23) were represented by grooves approximately 1/16 inch wide and 1/16 inch deep, cut into the surfaces as indicated. These tests were made with the propeller operating and with the model complete as shown in figure 19. Propeller tests were made first with the model surfaces aerodynamically smooth; later the simulated surface irregularities were added and similar tests were made.

All the values of propulsive efficiency given are based on the drag of the aerodynamically smooth airplane model with propeller removed and without rotation of the cowling nose. Figure 24 compares, for the condition $\beta = 55^{\circ}$, the effects of adding the retractable landing-gear cover plates and other surface irregularities to the aerodynamically smooth model. The drag increment due to addition of the landing-gear cover plates caused a decrease in η_{max} of about 1 percent. The influence of additional surface irregularities, such as rudder, elevator, canopy, and door joints, caused an additional decrease in propulsive efficiency of about 1.5 percent.

Gun Installations in Low-Drag Wing

Several wing-gun installations were tested to determine their effects on the aerodynamic characteristics of the complete airplane model with low-drag wing. For each installation three simulated guns were mounted in each wing. In one installation the blast tube and part of the gun barrel protrude ahead of the wing, as shown in figure 25. In another installation the guns were mounted wholly within the wing so that the forward tip of the barrel would be some distance behind the leading edge of the wing. Two types of opening in the leading edge were tested for this installation: type A opening designed to have minimum adverse effect (fig. 26), and type B opening which is merely a circular passage (fig. 27). All the openings tested had air flowing through them and exhausting from a single opening on the upper surface of each wing about 0.6 chord back from the leading edge. A detailed description of the investigation is given in reference 3.

The results showed that the installations tested have little effect on the maximum lift coefficient of the model. The effect on the drag coefficient was quite noticeable. The least adverse effect was obtained with the completely internal mounting and with type A opening: C_D at $C_L = 0.1$ was increased about 0.0001. Type B opening gave an increase of 0.0008, and the protruding type of installation increased C_D by 0.0007.

Comparative Drag of Original and of Completely Revised Pursuit Airplane Models

It is of considerable interest to note here that the measured drag of the actual full-scale pursuit airplane in flight condition, complete with all external protuberances, air scoops, and surface irregularities, was almost twice the drag of the smooth model of this airplane with all cooling air taken in at the cowling nose. A good indication is thus given of the gains that might be expected from elimination of surface irregularities, air leakage, and protuberances on the actual airplane. Every effort consistent with other required characteristics should therefore be made to develop aerodynamically clean airplanes.

It is also of interest to compare the drag, as measured in the wind tunnel, of the smooth original pursuit-

airplane model with the drag of the smooth completely revised pursuit model; the values are taken for the assumed high-speed lift coefficient, $C_L = 0.10$.

Original model with air flow, no propeller,
$C_D = 0.0137$

Revised model with air flow, no propeller,
$C_D = 0.0112$

In order to make the comparison valid, both coefficients should be based on the same wing area. It appears desirable to base the coefficients on the area of the original wing, and the change for the low-drag wing was made as follows:

C_{D_o} of wing from wake survey = 0.0042

C_{D_i} of wing = $(C_L^2/\pi R)$ = .0005

C_D of wing = .0047

Decrease area from 42.83 to 35.8 square feet,

ΔC_D (based on S = 42.83) = $\left(1 - \frac{35.8}{42.83}\right) \times 0.0047 = 0.00077$

C_D of model with reduced wing area (based on S=35.8)

$C_D = (0.0112 - 0.00077) \times \frac{42.83}{35.8} = 0.0126$

The drag coefficients then compare, for $C_L = 0.1$:

Original model with air flow, no propeller, 0.0137

Revised model with air flow, no propeller, .0125

An approximate calculation was made of the relative high speeds of the two airplanes based on the drag coefficient mentioned. If compressibility effects are neglected and a propeller efficiency of 0.80 is assumed with 1000 horsepower at 20,000 feet altitude, the following values are obtained:

Original pursuit airplane - - - - 414 miles per hour

Completely revised pursuit airplane - - - - - - - - - - - - - - - 424 miles per hour

Thus, the maximum difference in speed between the two airplanes would appear to be about 10 miles per hour with the 1000-horsepower engine. Because of other factors, such as surface irregularities due to manufacturing, this differential would probably be reduced. On the other hand, the original model will be affected by compressibility at the speeds mentioned and the revised airplane would not be affected and these effects would tend to increase the differential. The original smooth airplane will encounter critical compressibility effects at about 430 miles per hour. Obviously, with greater engine power and the required propeller, considerably higher speeds could be obtained with the completely revised pursuit airplane because compressibility effects would not be a limiting factor up to speeds above 500 miles per hour.

CONCLUSIONS

Based on the results of the investigation described in this report, the following conclusions may be drawn:

1. Important reductions in wing drag and important increases in compressibility speeds may be obtained by use of the NACA low-drag airfoil section.

2. A wing with NACA low-drag airfoil sections had lift and stalling characteristics that were similar to those of conventional wings, and the action of simple split flaps was about the same in increasing the lift.

3. The effect of the propeller slipstream, either for the idling condition or for thrust equal to drag, was to cause an increase in the drag of that portion of the low-drag wing in the slipstream to a value about the same as that of conventional wing sections without slipstream.

4. The new NACA high-speed cowling arrangement on the pursuit-airplane model tested indicated that satisfactory performance at high altitudes and speeds up to more than 500 miles per hour could be obtained before critical compressibility effects were encountered. When NACA cowling C was used, critical compressibility effects were indicated at 20,000 feet altitude at airplane speeds of about 430 miles per hour.

5. Propulsive efficiencies appear to be increased by

the use of the high-speed cowling at high values of V/nD compared with the efficiencies obtained with cowling C.

6. Adverse interference effects on critical compressibility speed caused by the wing-fuselage juncture were reduced to practically zero by proper shaping of the juncture.

7. The tests show the aerodynamic advantage of placing wing guns entirely within the wing.

Langley Memorial Aeronautical Laboratory,
National Advisory Committee for Aeronautics,
Langley Field, Va.

REFERENCES

1. Robinson, Russell G., and Becker, John V.: High-Speed Tests of Radial-Engine Cowlings. NACA confidential report, 1939.

2. McHugh, James G.: Progress Report on Cowlings for Air-Cooled Engines Investigated in the NACA 19-Foot Pressure Wind Tunnel. NACA advance restricted report, 1941.

3. Muse, Thomas C.: The Effect of Various Wing-Gun Installations on the Aerodynamic Characteristics of an Airplane Model Equipped with an NACA Low-Drag Wing. NACA confidential report, 1941.

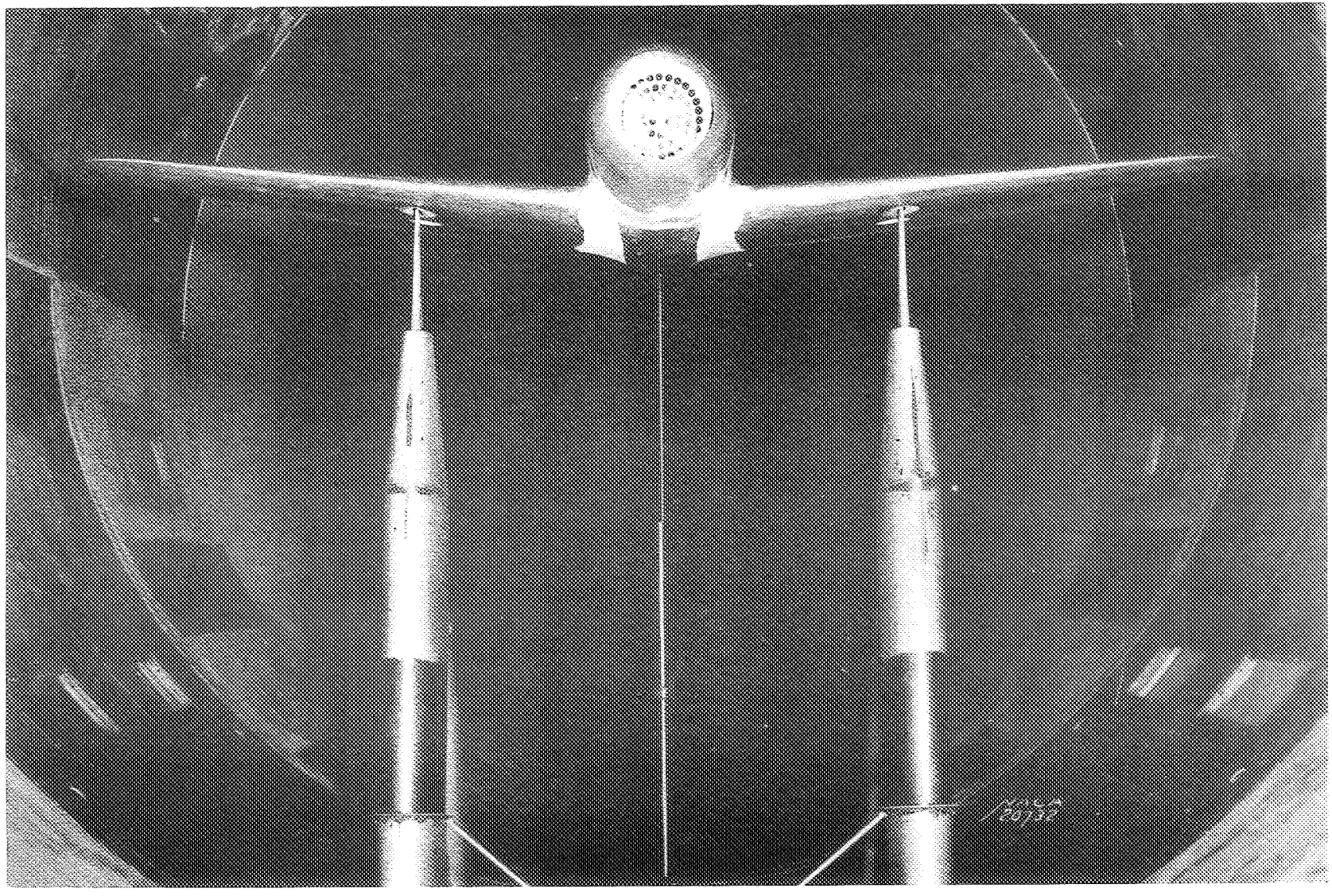

Figure 1.- The 0.4-scale model of the basic pursuit airplane in the 19-foot pressure tunnel.

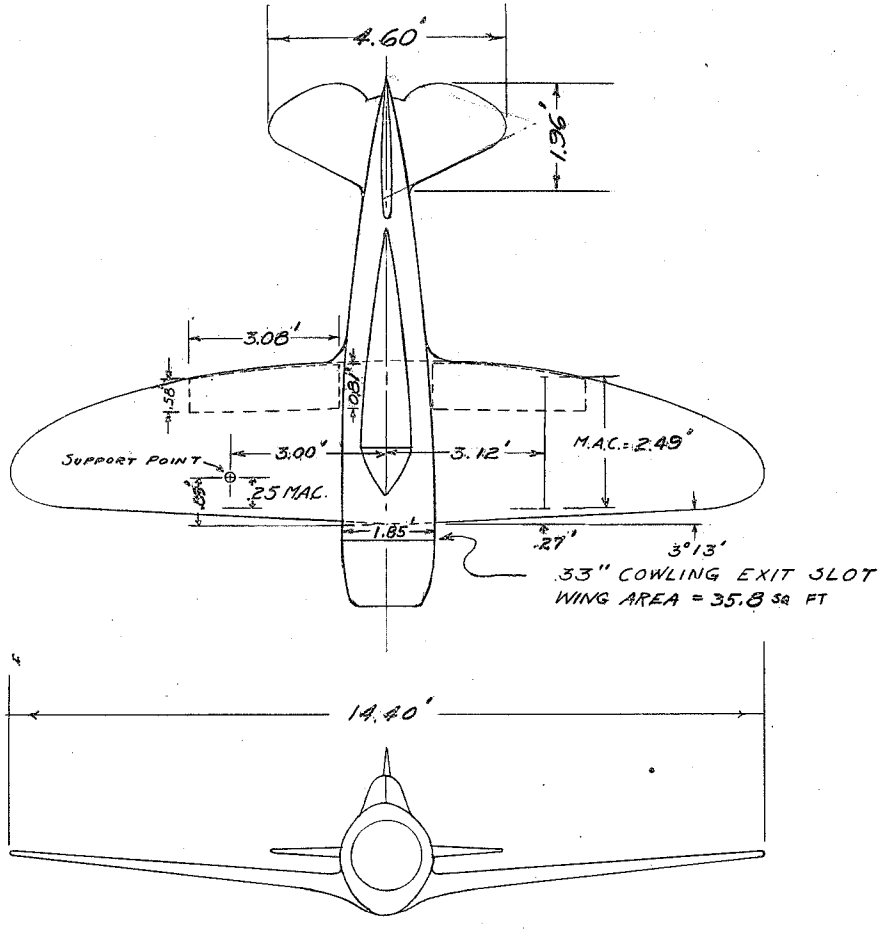

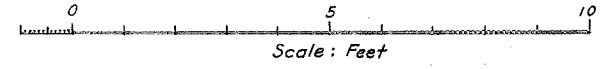

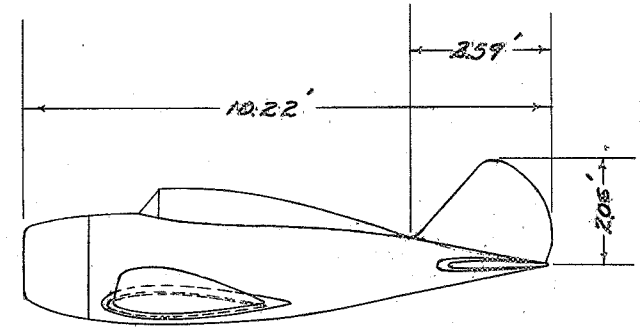

FIGURE 2.- PLAN AND ELEVATIONS OF 0.4-SCALE MODEL OF THE BASIC PURSUIT AIRPLANE.

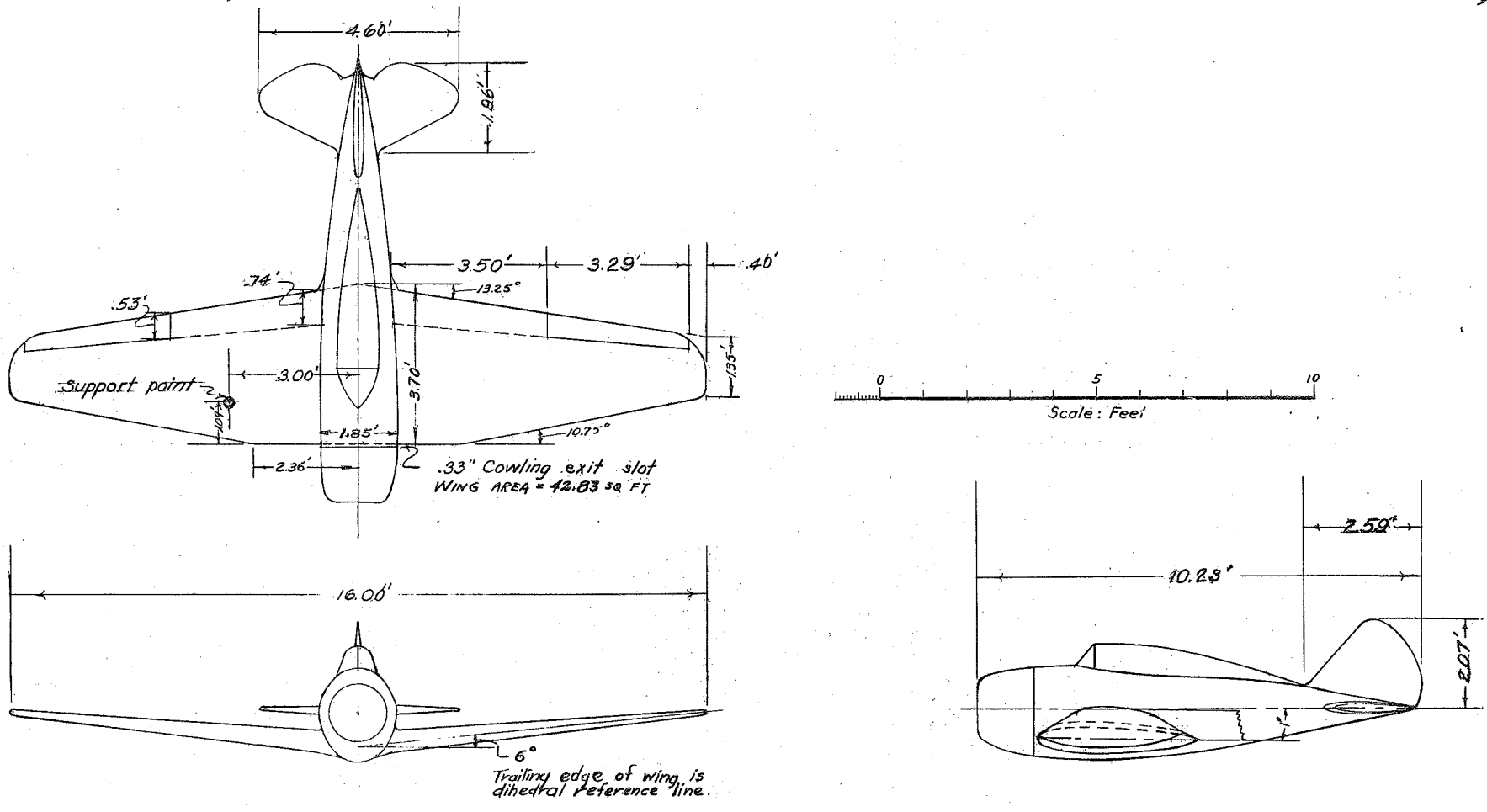

FIGURE 3.—PLAN AND ELEVATIONS OF 0.4 - SCALE MODEL OF THE PURSUIT AIRPLANE WITH NACA LOW-DRAG WING.

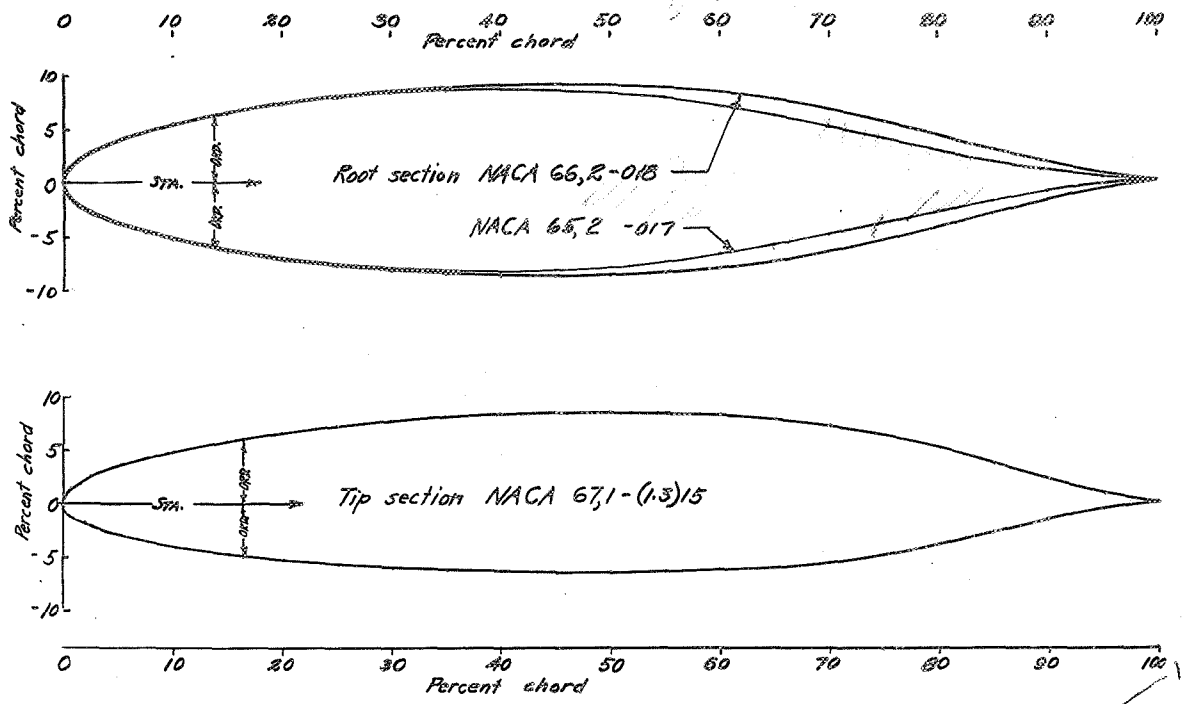

NACA 66,2-018	
Upper surface [1]	
Station	Ordinate
0	0
.5	1.438
.75	1.730
1.25	2.180
2.5	2.938
5.	3.984
7.5	4.804
10.	5.486
15.	6.541
20.	7.342
25.	7.957
30.	8.419
35.	8.741
40.	8.933
45.	8.998
50.	8.936
55.	8.713
60.	8.316
65.	7.629
70.	6.657
75.	5.533
80.	4.302
85.	3.027
90.	1.789
95.	.672
100.	0.

NACA 65,2 - 017	
Upper surface [1]	
Station	Ordinate
0	0
.5	1.277
.75	1.512
1.25	1.908
2.5	2.664
5.0	3.764
7.5	4.586
10.	5.264
15.	6.330
20.	7.120
25.	7.705
30.	8.125
35.	8.381
40.	8.495
45.	8.434
50.	8.152
55.	7.629
60.	6.903
65.	6.000
70.	4.986
75.	3.976
80.	2.936
85.	1.909
90.	1.043
95.	.361
100.	.00

[1] Lower surface symmetrical

NACA 67,1-(1.3)15			
Upper surface		Lower surface	
Station	Ordinate	Station	Ordinate
0	0	0	0
.422	1.209	.578	-1.129
.663	1.450	.837	-1.340
1.15	1.845	1.35	-1.675
2.39	2.547	2.61	-2.245
4.88	3.504	5.13	-2.998
7.37	4.247	7.63	-3.559
9.87	4.855	10.13	-4.013
14.88	5.840	15.12	-4.736
19.89	6.597	20.11	-5.281
24.90	7.208	25.10	-5.722
29.92	7.673	30.08	-6.051
34.94	8.022	35.06	-6.296
39.96	8.263	40.04	-6.463
44.98	8.393	45.02	-6.549
50.00	8.426	50.00	-6.566
55.02	8.342	59.98	-6.498
60.05	8.125	59.95	-6.351
65.08	7.752	64.92	-6.046
70.11	7.188	69.89	-5.620
75.14	6.281	74.87	-4.927
80.12	5.061	79.88	-3.965
85.09	3.666	84.91	-2.850
90.06	2.207	89.93	-1.677
95.02	.864	94.98	-.614
100.	0.	100.	0.

FIGURE 4.— Airfoil sections of root and tip for NACA low-drag wing.

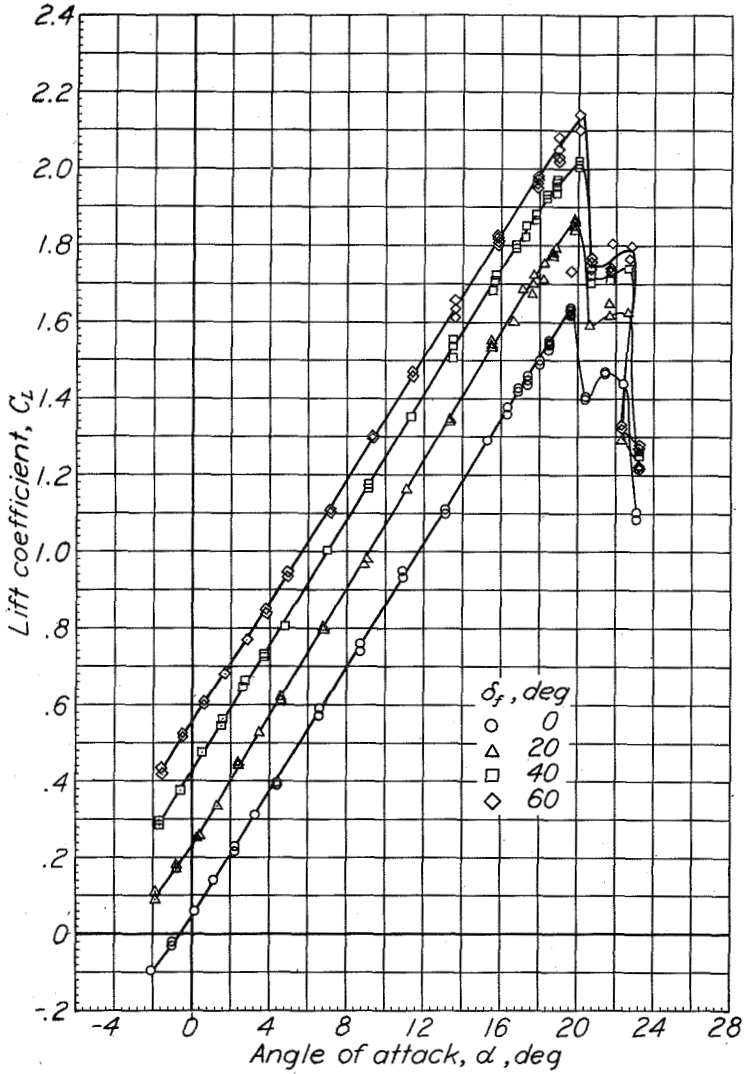

Figure 5.- Lift coefficients obtained with conventional wing and partial-span split flaps on basic pursuit-airplane model. R,4.8 x 10^6.

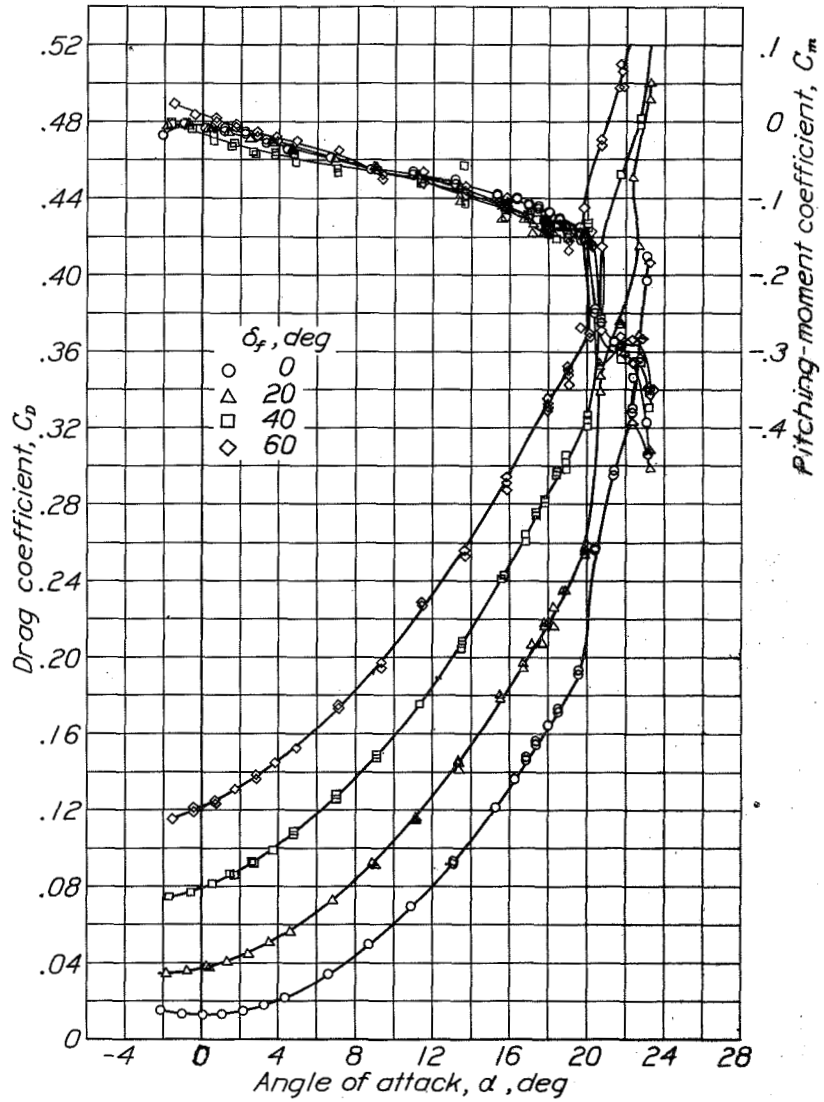

Figure 6.- Drag and pitching-moment coefficients obtained with conventional wing and partial-span split flaps on basic pursuit-airplane model. R,4.8 x 10^6.

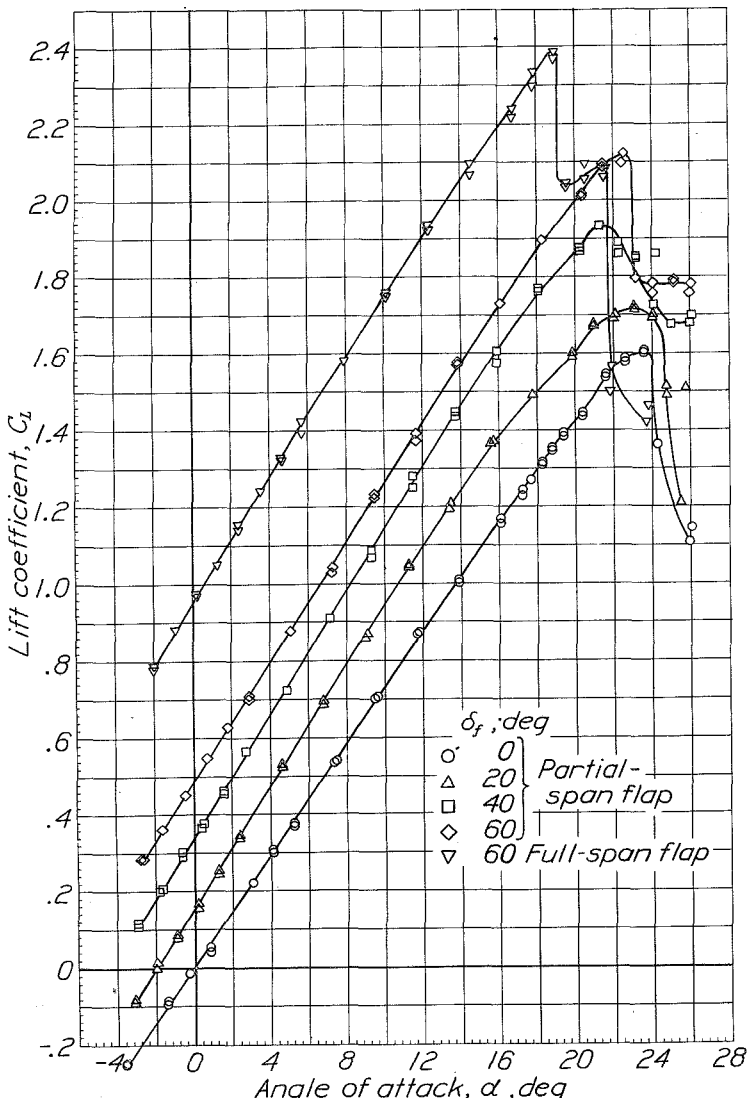

Figure 7.- Lift coefficients obtained with NACA low-drag wing and partial-span and full-span split flaps on pursuit-airplane model. R,5.5 x 10^6.

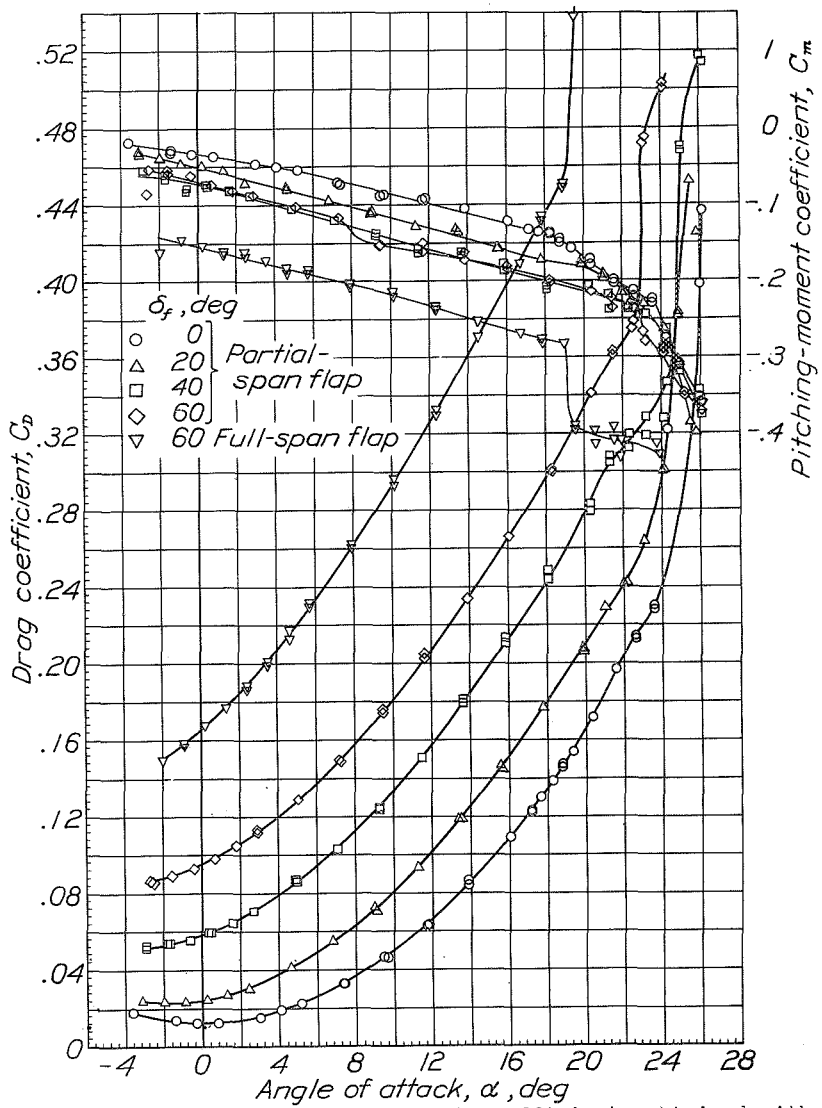

Figure 8.- Drag and pitching-moment coefficients obtained with NACA low-drag wing and partial-span and full-span split flaps on pursuit-airplane model. R,5.5 x 10^6.

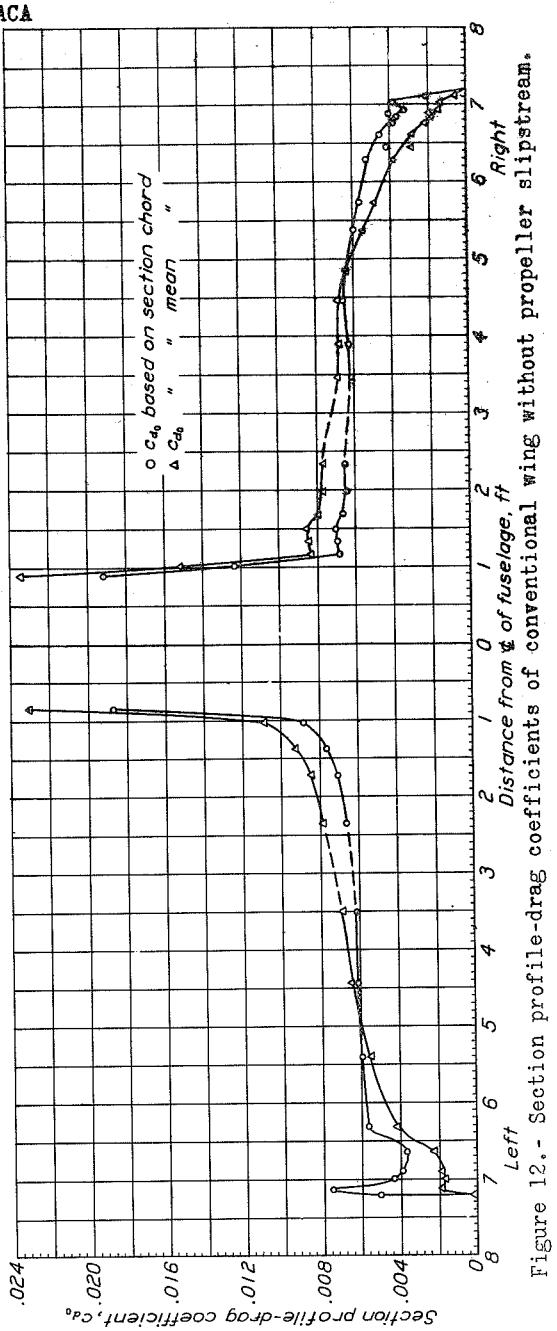

Figure 12.- Section profile-drag coefficients of conventional wing without propeller slipstream.

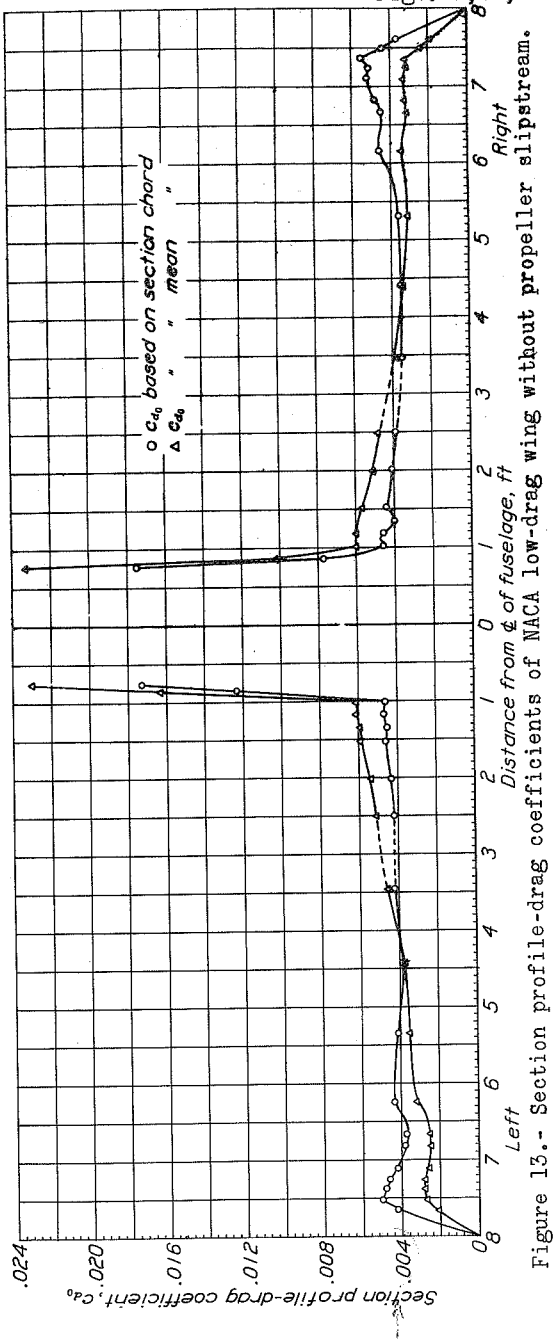

Figure 13.- Section profile-drag coefficients of NACA low-drag wing without propeller slipstream.

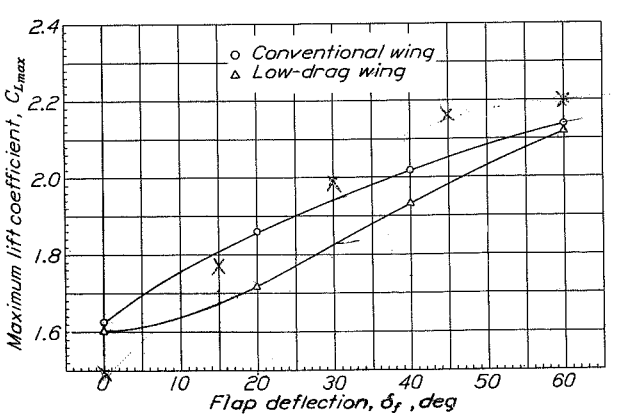

Figure 9.- Effect of deflection of partial-span split flap on $C_{L_{max}}$ of pursuit-airplane model with conventional wing and with NACA low-drag wing.

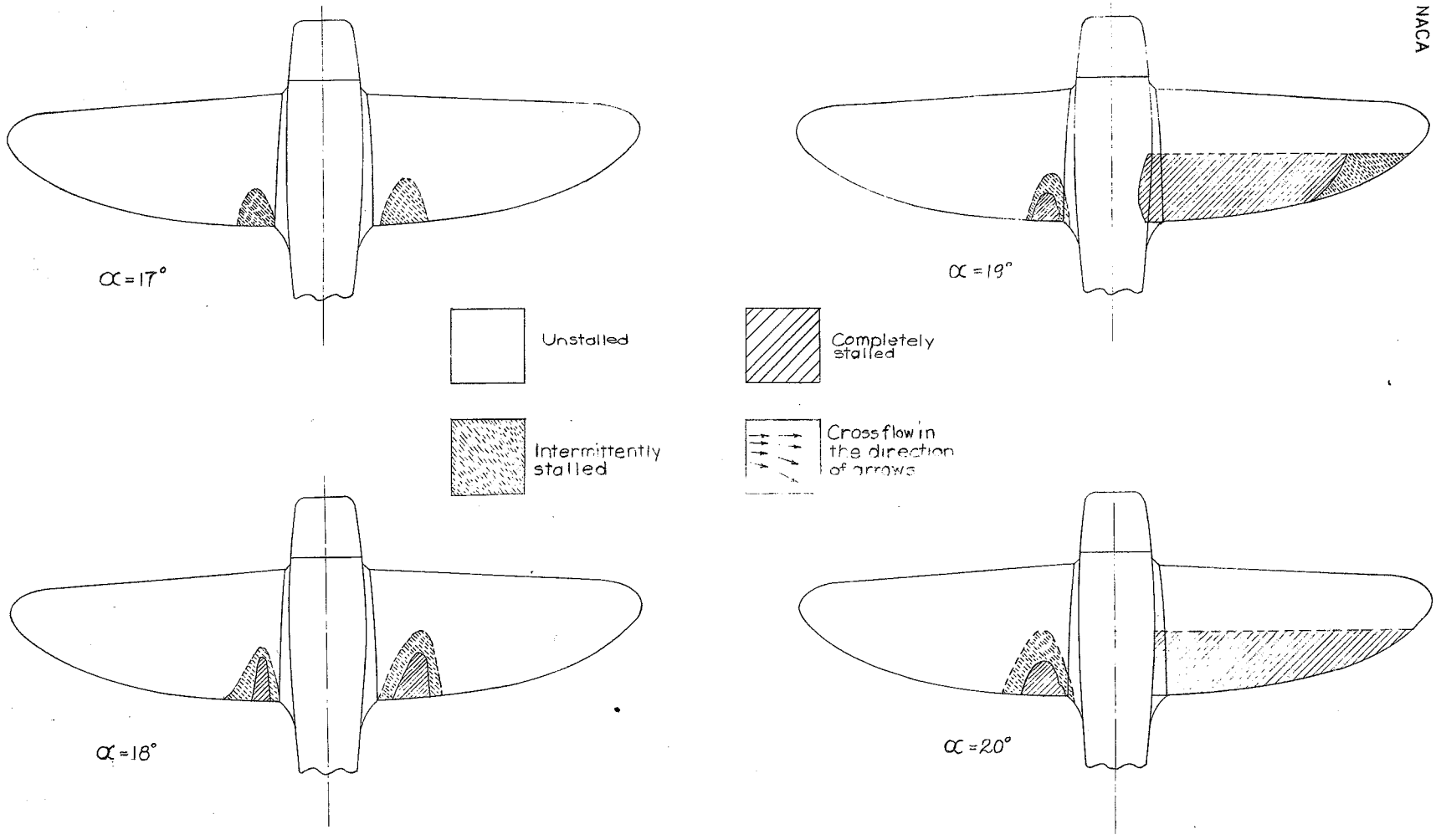

(a) Flap neutral.

FIGURE 10.- Stall diagrams of the conventional wing on basic model of pursuit airplane.

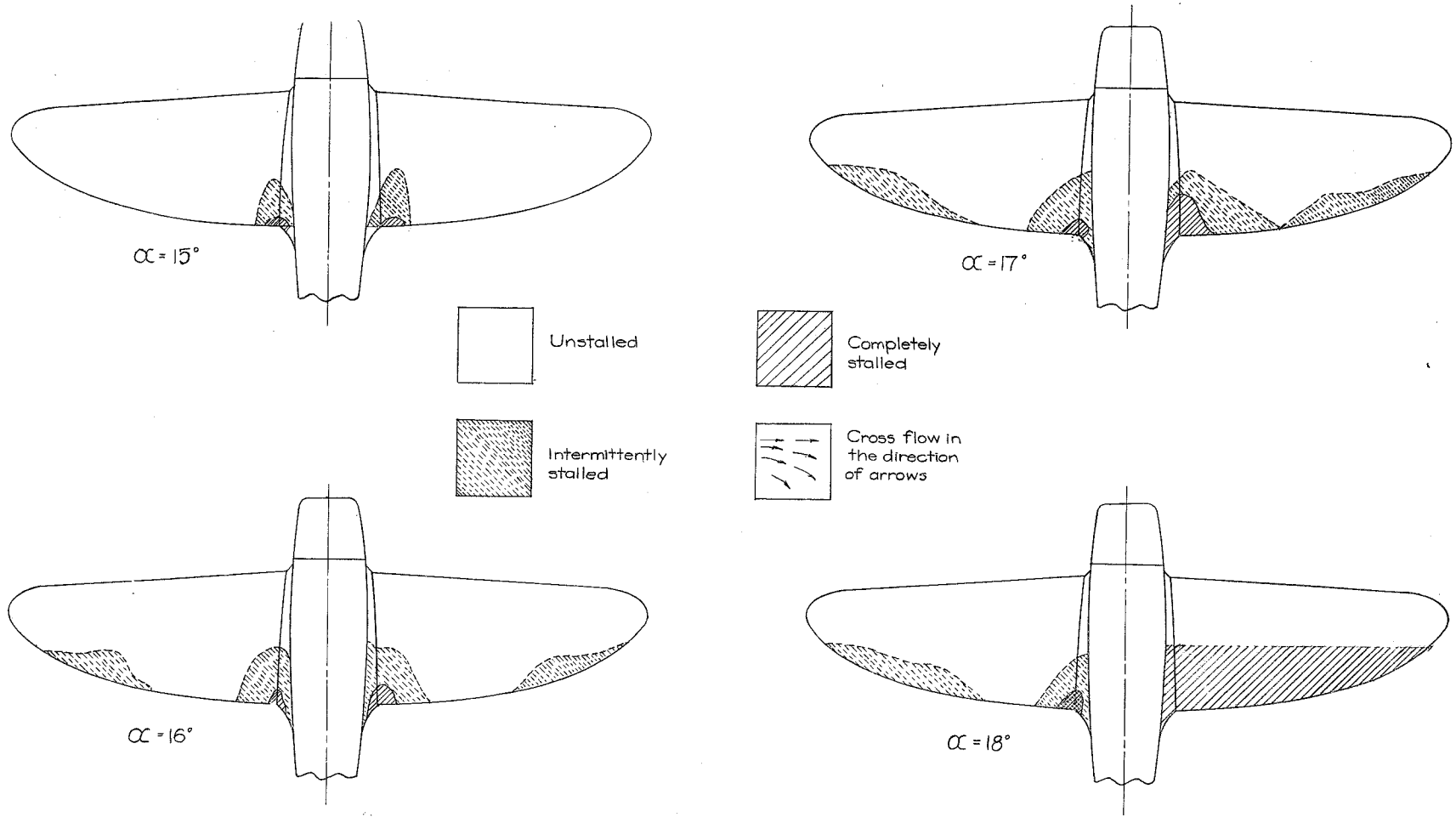

(b) Partial-span split flap deflected 60°.

Figure 10.- Stall diagrams of the conventional wing on basic model of pursuit airplane.

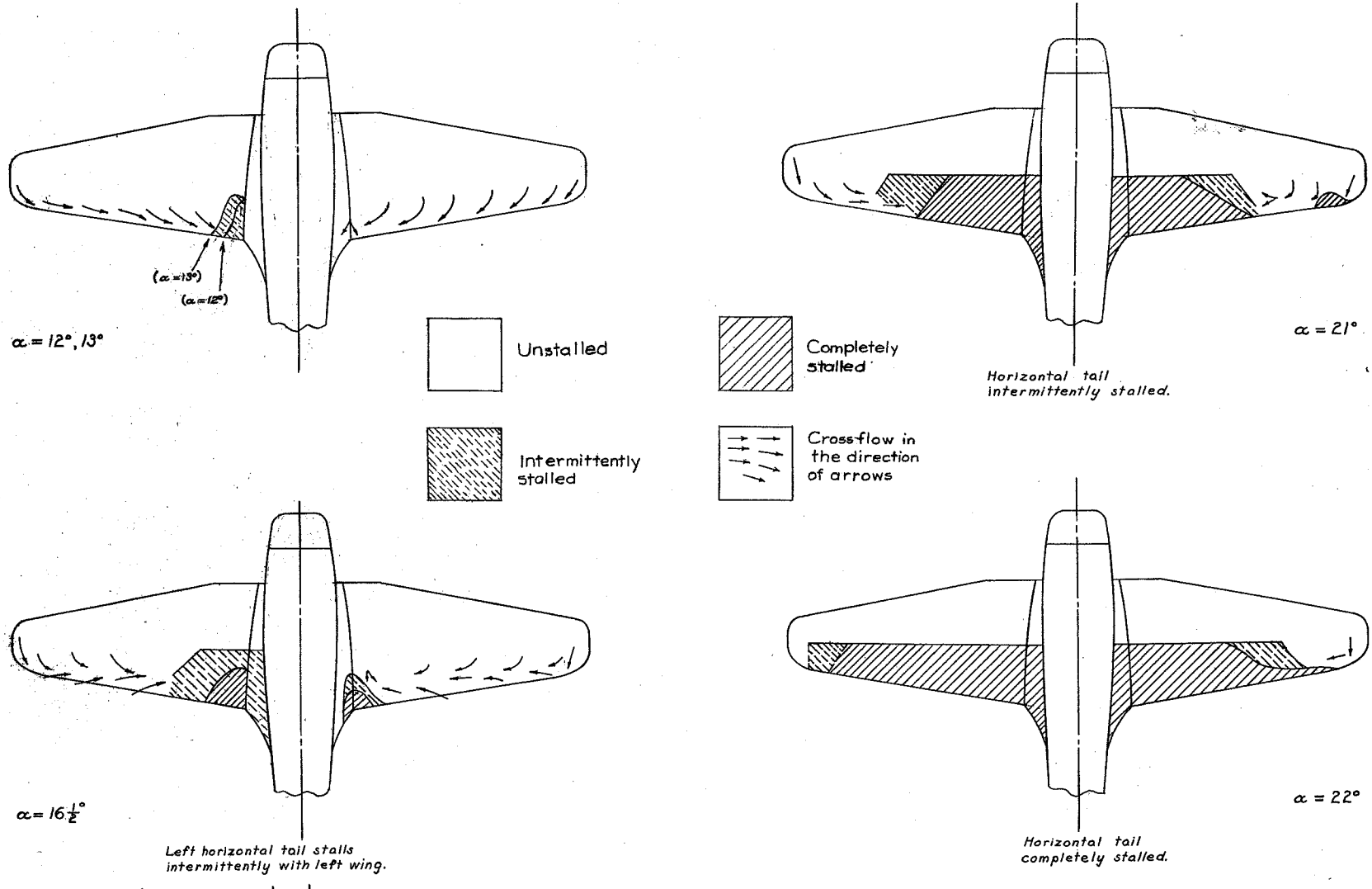

(a) Flap neutral.

Figure 11.—Stall diagrams of NACA low-drag wing on model of pursuit airplane.

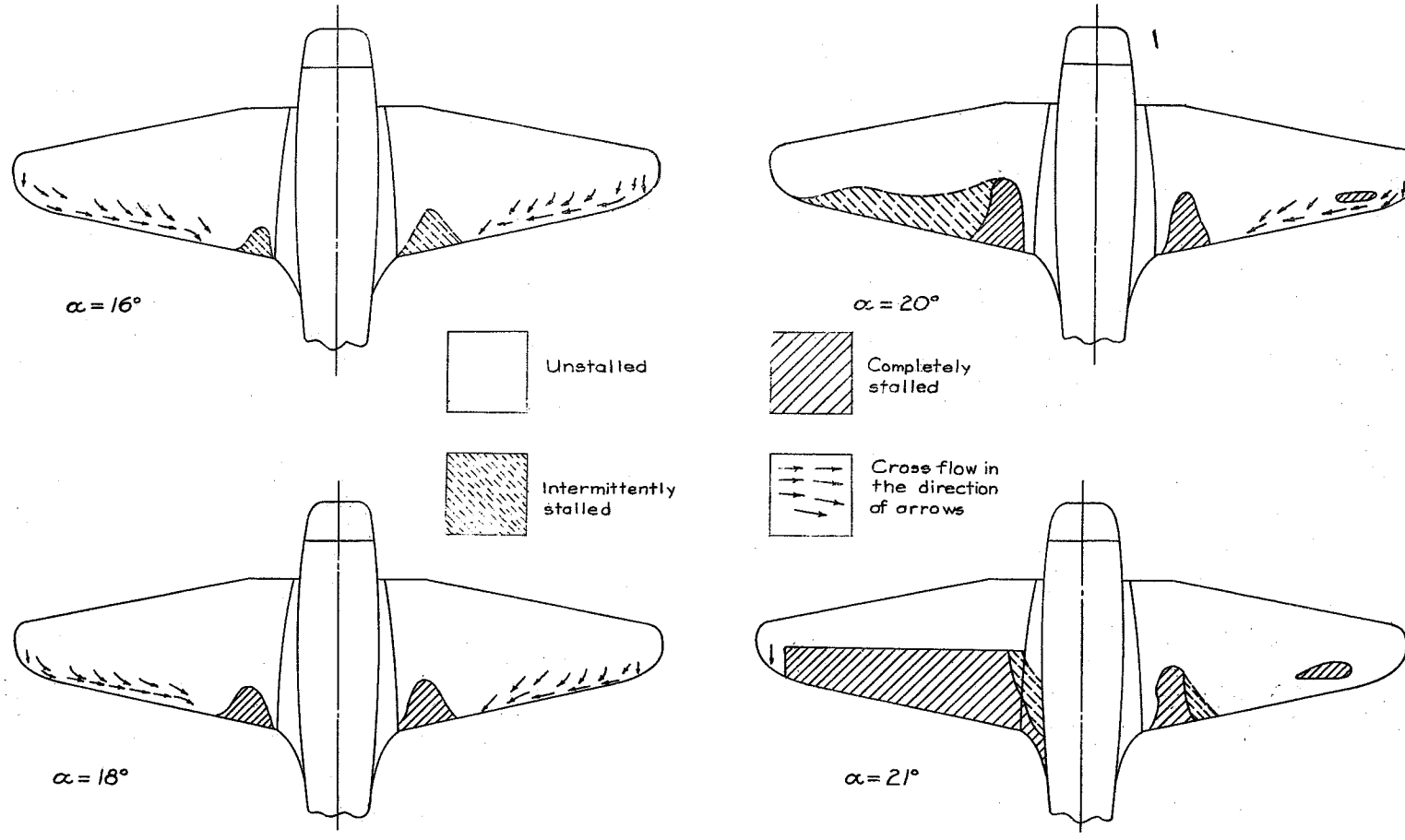

(b) Partial-span split flap deflected 60°.

Figure 11. — Stall diagrams of NACA low-drag wing on model of pursuit airplane.

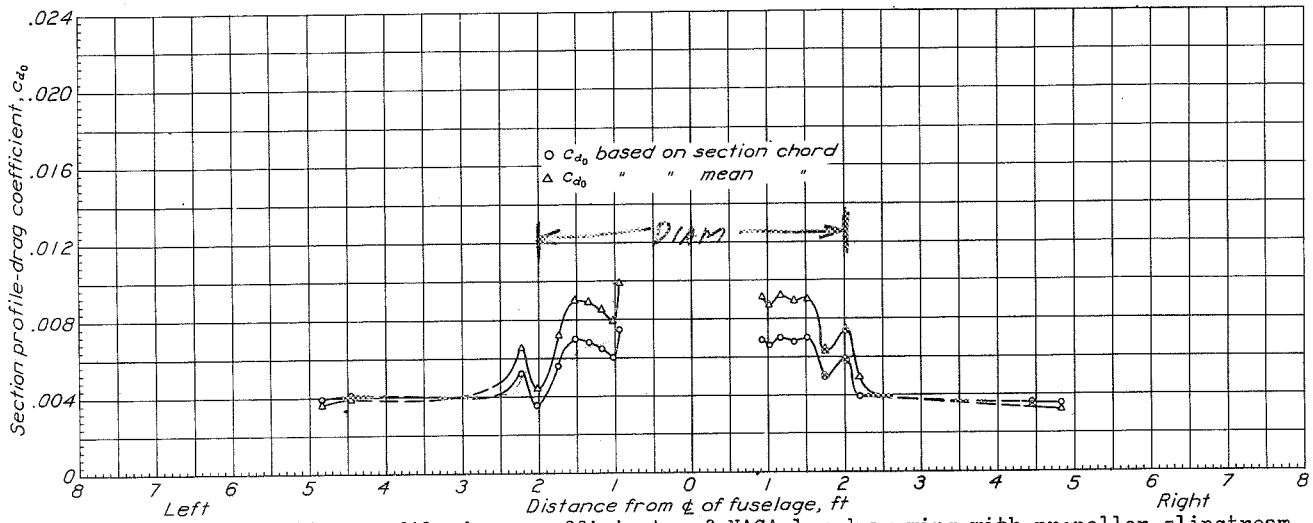

Figure 14.- Section profile-drag coefficients of NACA low-drag wing with propeller slipstream.

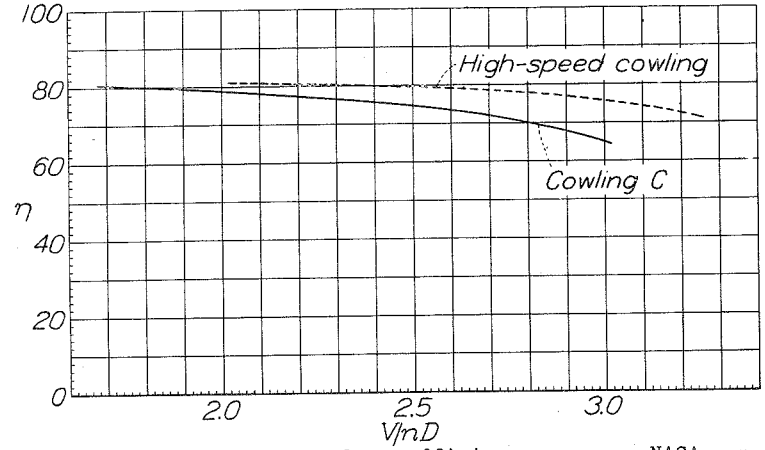

Figure 17.- Propeller envelope efficiency curves. NACA conventional cowling C and NACA high-speed cowling on pursuit-airplane model.

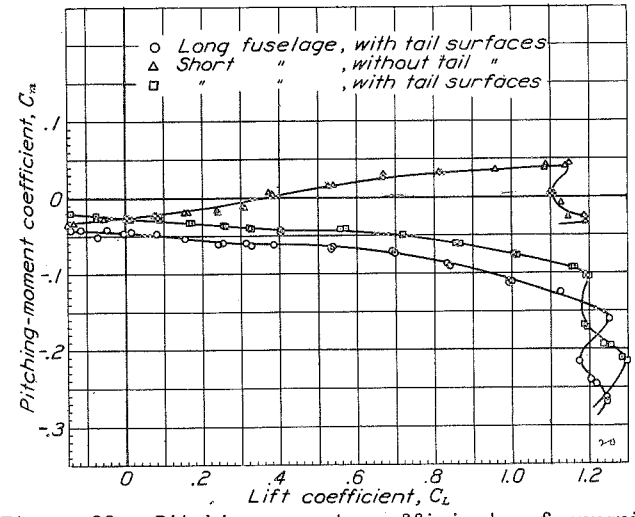

Figure 20.- Pitching-moment coefficients of pursuit-airplane model for various fuselage and tail conditions.

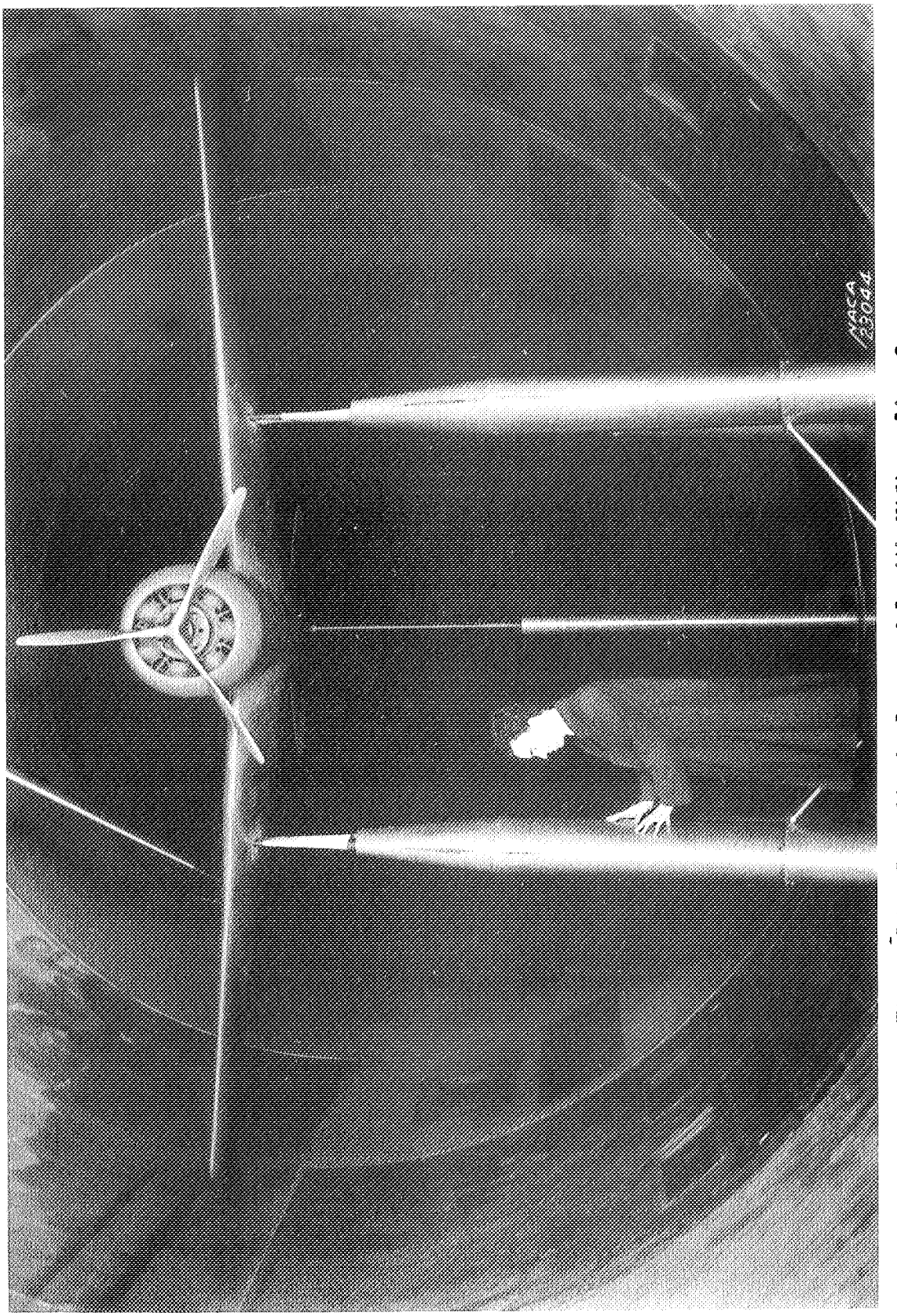

Figure 15.- Pursuit-airplane model with NACA cowling C.

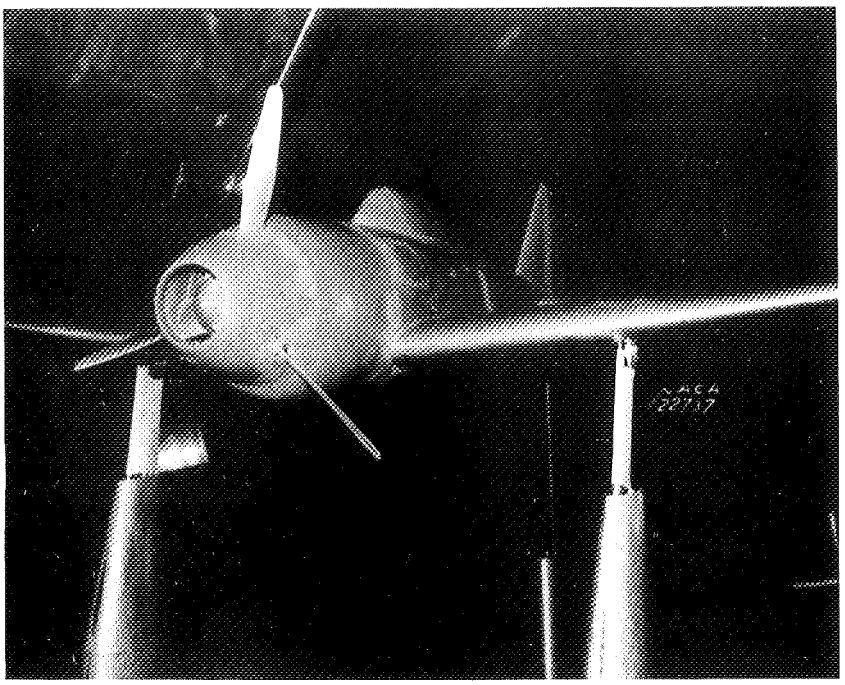

Figure 16.- Pursuit-airplane model with NACA high-speed cowling.

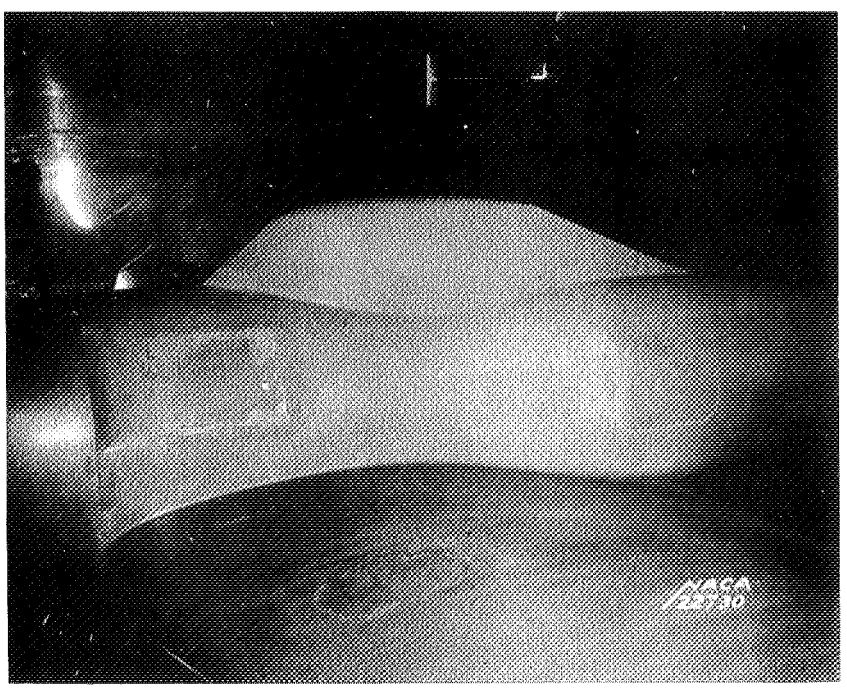

Figure 23.- Simulated door, canopy, and inspection plate joints on short fuselage of pursuit-airplane model.

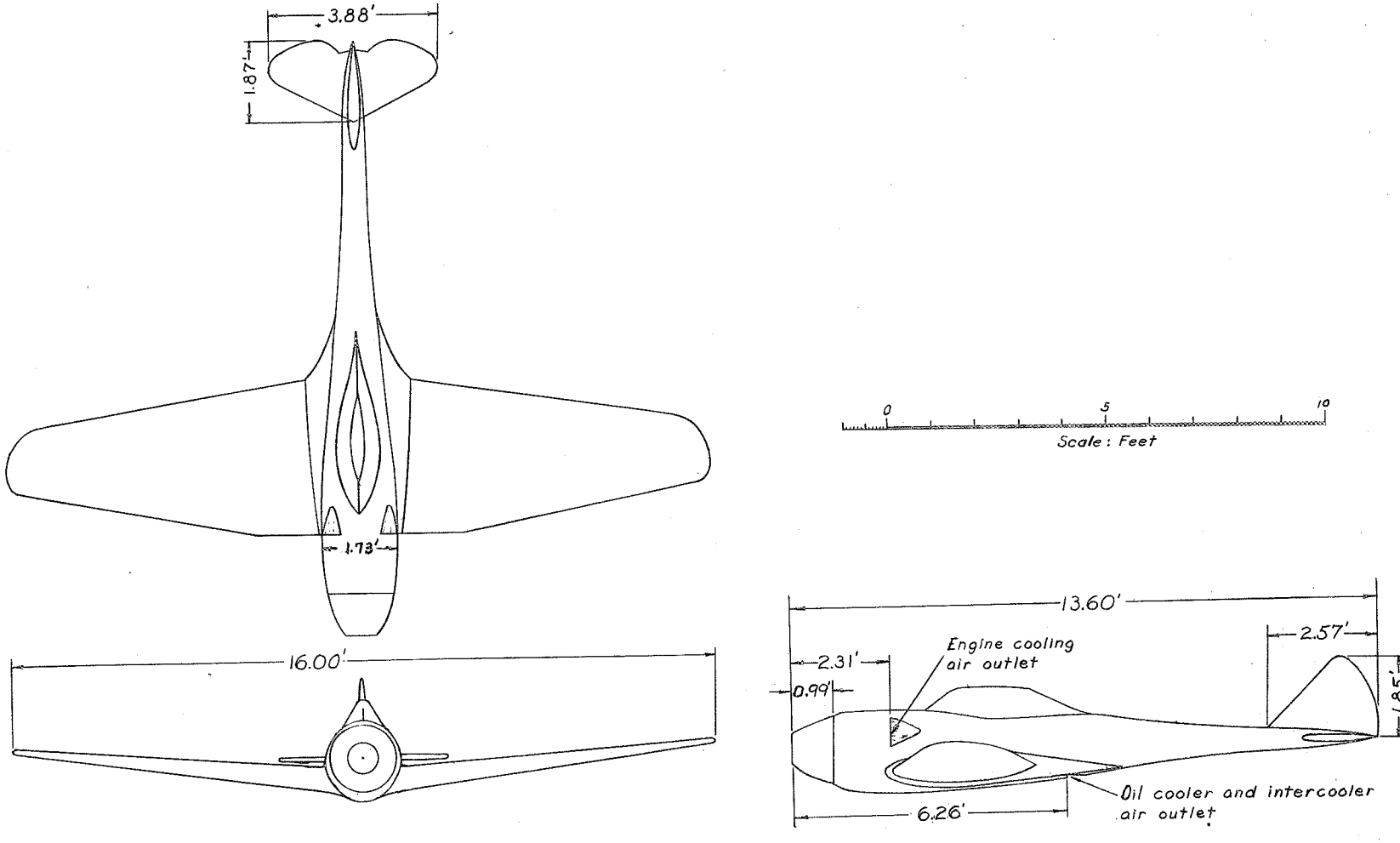

FIGURE 18 - Pursuit-airplane model with long fuselage and small tail.

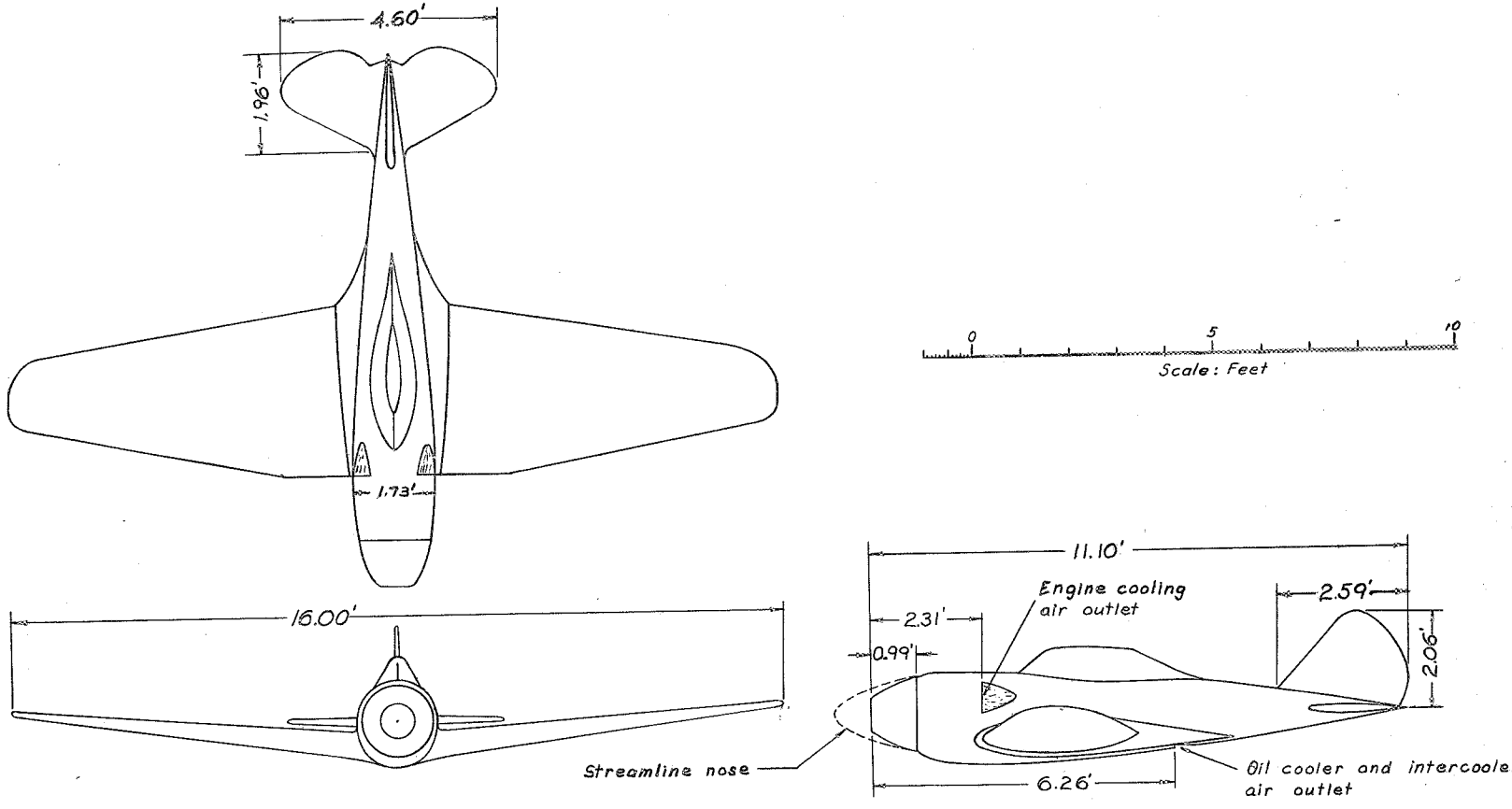

FIGURE 19.-Pursuit-airplane model with short fuselage and large tail.

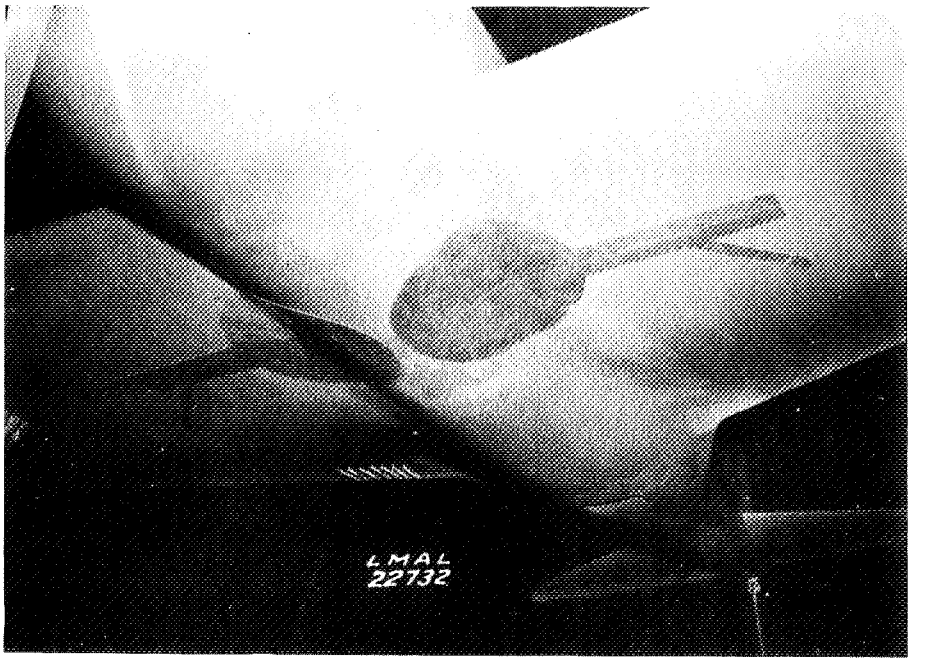

Figure 21.- Simulated retractable landing-gear cover plates on low-drag wing of pursuit-airplane model.

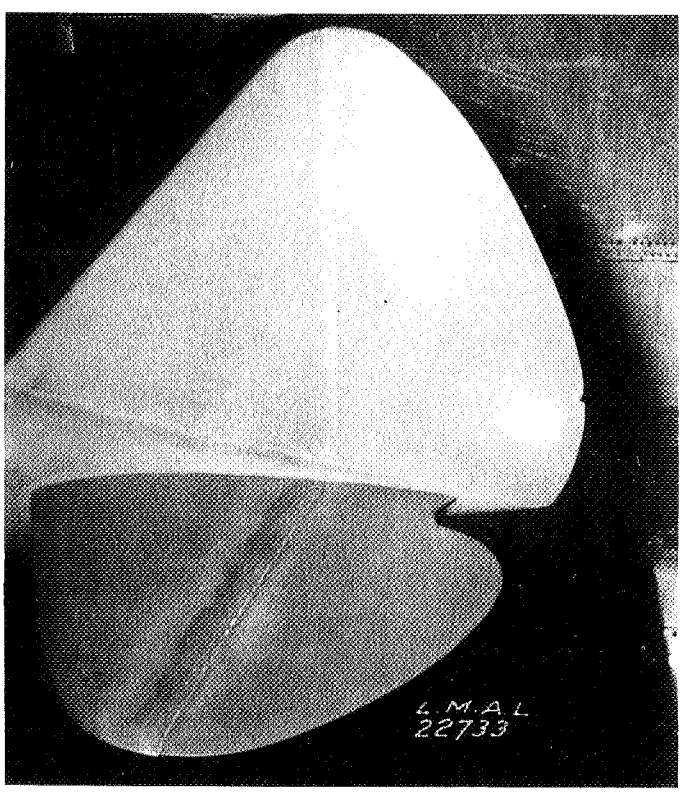

Figure 22.- Simulated rudder and elevator sealed hinge joints on tail surfaces of pursuit-airplane model.

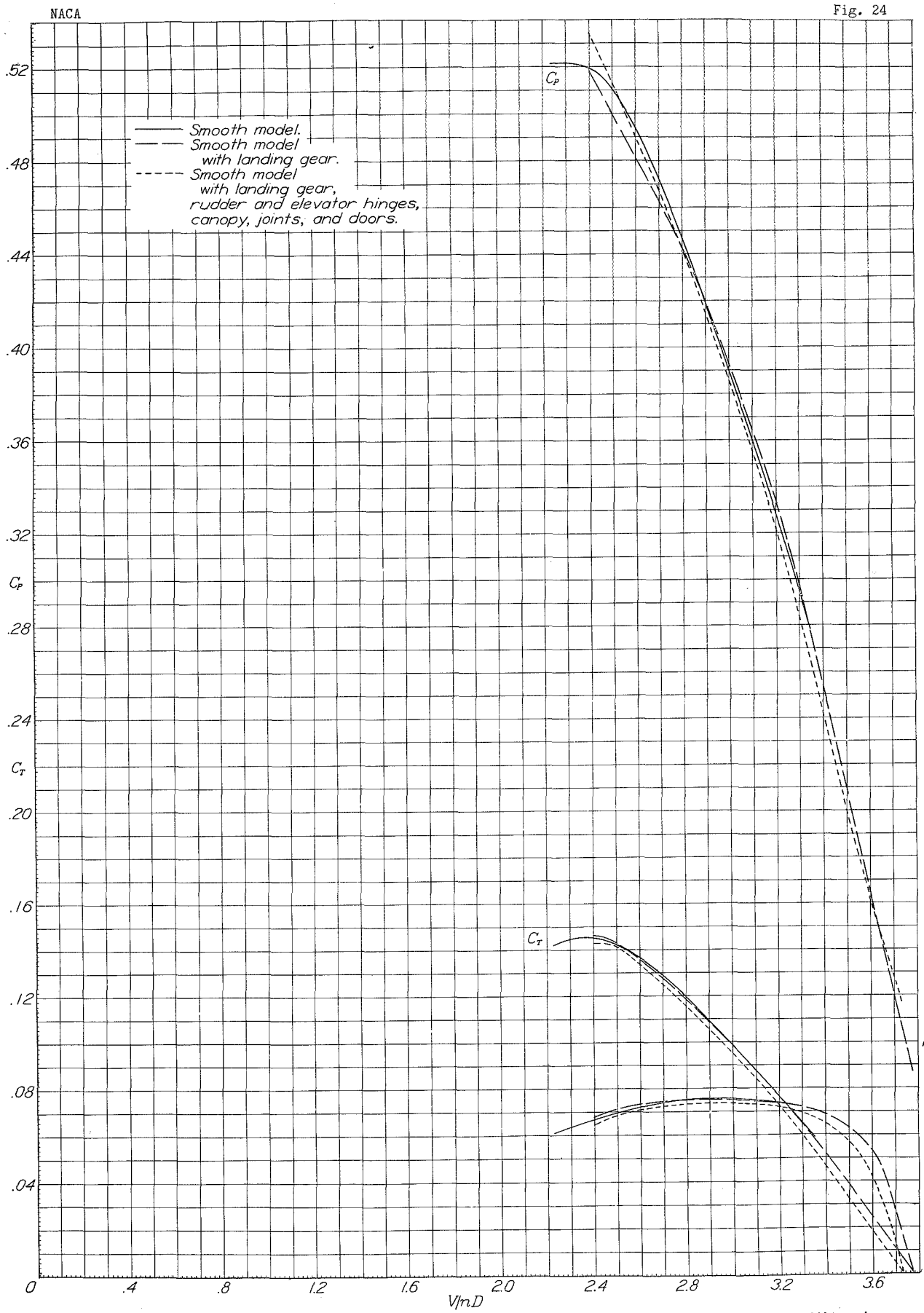

Figure 24.- Comparison of propeller characteristics obtained from tests of pursuit-airplane model with various surface irregularities. β,55°.

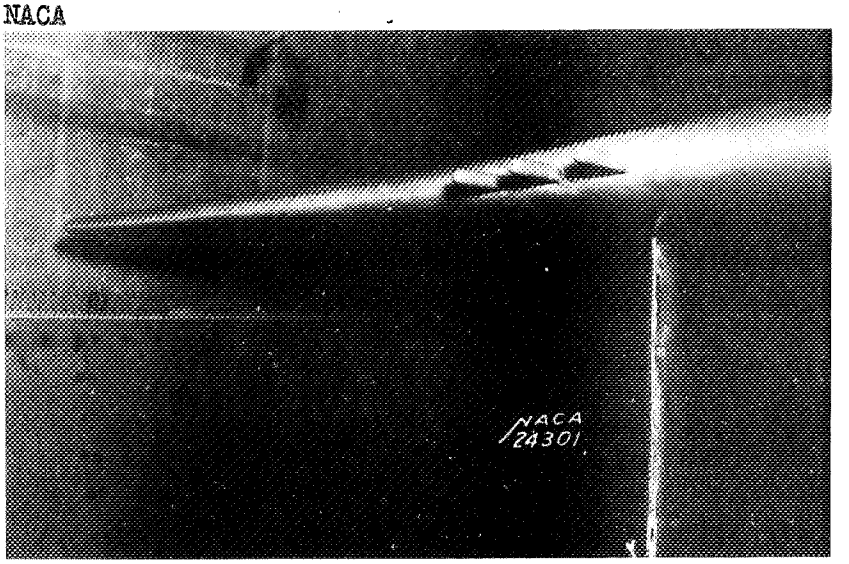

Figure 25.- Protruding gun installation in low-drag wing of pursuit-airplane model.

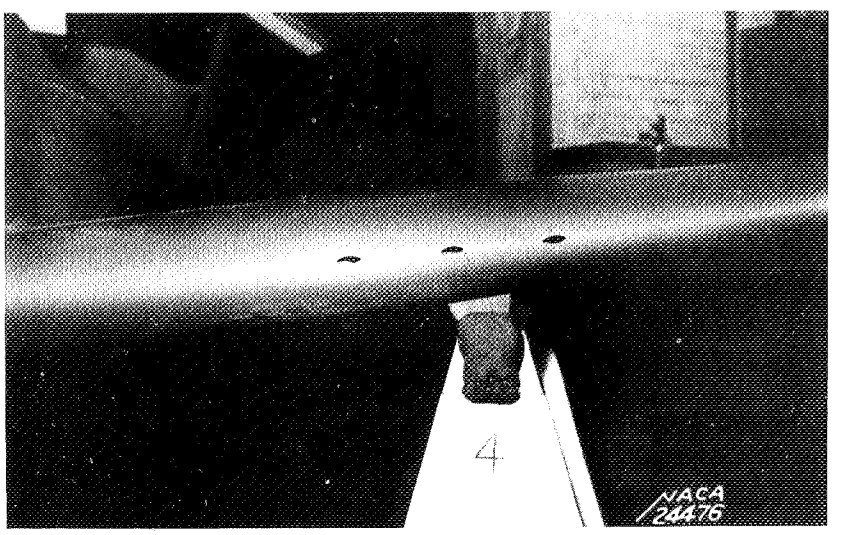

Figure 26.- Submerged gun installation with type A opening in low-drag wing of pursuit-airplane model.

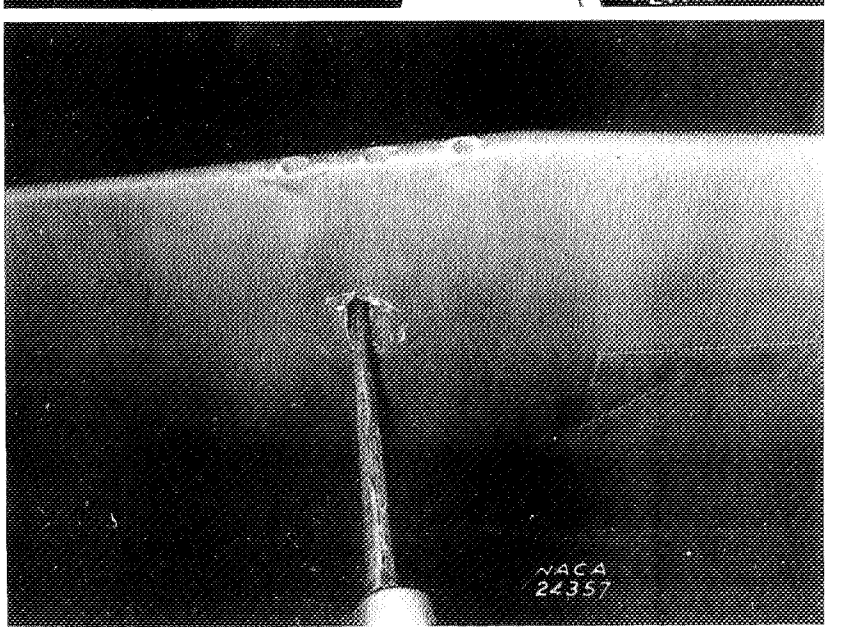

Figure 27.- Submerged gun installation with type B opening in low-drag wing of pursuit-airplane model.